Proceedings of ISFOG 2025
5TH INTERNATIONAL SYMPOSIUM ON
FRONTIERS IN OFFSHORE GEOTECHNICS
Nantes, France | June 9-13 2025
© 2025 the Authors
ISBN 978-2-85782-758-0

Rate effects in circular footing penetration in saturated sand

S. H. Chow*
The University of Melbourne, Australia

B. Bienen, M.F. Randolph
Centre for Offshore Foundation Systems, University of Western Australia, Perth, Australia

T. Continibali
Formerly University of Western Australia, Perth, Australia

shiaohuey.chow@unimelb.edu.au (corresponding author)

ABSTRACT: This study investigates rate effects in the penetration resistance of a circular footing into saturated sand using laboratory 1g and centrifuge tests. A model circular footing of 40 mm diameter was pushed at various penetration velocities into fine silica sand saturated with either water or a highly viscous pore fluid. The highly viscous pore fluid, water with Methocel™ cellulose ether, with a dynamic viscosity of 480 mPa.s was used to reduce the Darcy permeability of the sand sample in order to achieve partially drained and undrained conditions. The 1g model tests were conducted in sand with a relative density of 45% to provide appropriately scaled dilational properties as compared with those obtained from centrifuge tests at 50g in the same sand at a typical field relative density of 76%. The 1g test results showed an increasing penetration resistance with increasing penetration velocity as the response became increasingly undrained. The observed rate effects in the penetration resistance are captured using a backbone curve framework. However, comparison between the 1g and 50g tests reveals difficulty in matching the response between the two stress levels, revealing uncertainty in existing stress scaling approaches.

Keywords: circular footing, sand, 1g tests, centrifuge tests, stress level effects

1 INTRODUCTION

Rapid soil-structure interaction is often encountered in offshore energy applications providing motivation for studies on rate effects in saturated sand (e.g. Palmer, 1999, Bransby and Ireland, 2009, Chow et al., 2018, 2022). In particular, rapid penetration of foundations and penetrometers in dilating sand has shown to cause 50 to 350% increase in sand resistance, as the sand consolidation condition changes from drained to undrained in centrifuge studies (Chow et al., 2022). The significant increase in sand resistance could cause undesired consequences, such as failure of offshore plough pulling system (Palmer, 1999).

Recent research on rate effects in sand have shown that this change in sand resistance with consolidation condition can be captured using a backbone curve framework (e.g. Finnie and Randolph, 1994, Chow et al. 2020). The consolidation condition is defined using a non-dimensional velocity term, $V = vd/c_v$ where v is the penetration velocity, d the nominal dimension of the structure (e.g. footing diameter) as a proxy for the drainage path length and c_v the coefficient of consolidation. As V increases (associated with either an increase in v and/or d, or a decrease in c_v), the consolidation condition will evolve from drained to partially drained to undrained. The backbone curve framework has been applied to different applications (piezocone, spudcan and plate anchor), with a range of rate parameters fitted for the different applications (Chow et al., 2022). To extend these studies, the rate effects in penetration resistance of a circular footing were investigated using 1g and 50g (centrifuge) model tests. The footing was pushed at various velocities into fine silica sand saturated with either water or a highly viscous pore fluid. The 1g tests also adopted a stress-scaling technique by testing at a lower relative density than the field density. The effectiveness of the stress-scaling technique was evaluated using the equivalent centrifuge tests at 50g.

2 EXPERIMENTAL DETAILS

2.1 Sand properties and preparation

The sand investigated in the study is a commercially available fine silica sand with properties summarised in Table 1 (Chow et al., 2019). Six samples were prepared in square or rectangular steel containers (1 m wide x 1 m long x 0.48 m high for Sample 1; and 0.39 m wide x 0.65 m long x 0.325 m high for the remaining

samples) via dry pluviation technique using an automated sand rainer. Depending on the gravitational acceleration (N) during testing, the specimens are either 45 to 47% (N = 1g) or 76% to 79% (N = 50g) in relative density (D_r) (see test program in Table 2). The lower D_r for the 1g samples is to account for the stress level effects, in which a stress scaling approach was applied using Bolton's (1986) stress-dilatancy framework (e.g. LeBlanc et al., 2010). The 1g sample with D_r = 45% is expected to yield a similar relative dilatancy index (I_R) of 4.87 to the 50g sample with D_r = 76% (Figure 1), considering mean effective stresses, p' = 0.07 and 6.7 kPa at 1g and 50g respectively. The mean effective stress, $p' = \sigma'_v(1+2K_0)/3$, is determined by considering the vertical effective stresses at normalised depth, z/d = 0.5 in the circular footing tests (σ'_v = 0.2 and 10.4 kPa at 1g and 50g respectively) and Coefficient of lateral earth pressure, K_0 = 1- sin ϕ'_{cs}, where ϕ'_{cs} = 31.9° (Table 1).

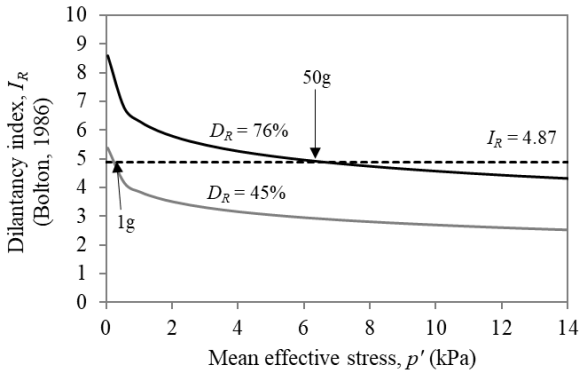

Figure 1. Stress scaling approach using equivalent relative dilatancy index (Bolton, 1986)

The specimens were saturated with either water or a viscous pore fluid (water solution with 2.2% concentration of Methocel™ cellulose ether Grade F450, Dow, 2002) through gravity feed from the base of soil container (Chow et al., 2018). A free fluid layer of 40 mm was maintained above the sand surface during testing. The viscous pore fluid (with dynamic viscosity $\mu_{methocel}$ ~ 480 mPa.s at 20°C) was used to reduce the Darcy permeability of the sand to achieve partially drained and undrained conditions in sand, which is a well-established physical modelling technique (e.g. Chow et al., 2019, Robinson et al., 2018).

Table 1. UWA SF silica sand properties (Chow et al., 2019).

Specific gravity, G_s	2.67
Particle size, d_{10}, d_{50}, d_{60}	0.12, 0.18, 0.19 mm
Minimum dry density, ρ_{min}	1497 kg/m^3
Maximum dry density, ρ_{max}	1774 kg/m^3
Critical state friction angle, ϕ'_{cs}	31.9° (triaxial)

2.2 Model circular footing

The aluminium model circular footing (Figure 2) is 40 mm in diameter (d) and has a height (h) of 45 mm. The height, higher than typically expected in practice, was selected to avoid flow-around of sand particles at deeper embedment for ease of interpreting the rate effects on the penetration resistance. Above this, the footing has a thin shaft of 10 mm for connection to the actuator. The footing is instrumented with a 1 MPa pore pressure transducer (PPT) at the middle of its base as shown in Figure 2.

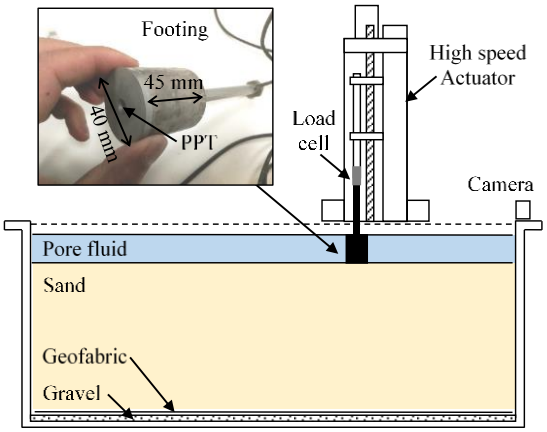

Figure 2. Model test setup and model circular footing

2.3 Experimental details

The 1g and 50g model tests were conducted at the National Geotechnical Centrifuge Facility (NGCF) at the University of Western Australia. The 50g centrifuge tests were conducted on a 3.6 m diameter beam centrifuge.

The test setup is presented in Figure 2. The test involves pushing the model footing into the sand using an actuator at a constant penetration velocity (v) ranging between 0.4 and 100 mm/s. A spacing of 5d was provided between the footing tests and rigid boundary to remove boundary effects (Bolton and Gui, 1993). The footing penetration resistance was measured using a load cell connected on top on the shaft of the footing, while the displacement is measured using the encoder of the actuator.

The test programme in summarised in Table 2. The test can be identified as SnP, where 'S' refers to test type ('L' for laboratory 1g test and 'C' for centrifuge test), 'n' denotes the non-dimensional velocity, V and 'P' denotes the pore fluid ('W' for water and 'M' for methocel). The non-dimensional velocity, $V = (vd/c_v)(\mu_{methocel}/\mu_{water})$, is computed for each test by considering the coefficient of consolidation (c_v) at the relevant stress level and relative density. The c_v of water-saturated sand was determined using Rowe cell tests (Chow et al. 2019).

Table 2. Model footing test programme

Sample (S) details[1]		Test ID	$\mu_{methocel}$ (mPa.s)	v (mm/s)	$V = (vd/c_v)$ $(\mu_{methocel}/\mu_{water})$
N = 1g	S1	L0.7W	1	1	0.7
D_r = 45%		L7W	1	10	7
γ' = 9.87		L68W	1	94	68
kN/m^3		L91W	1	127	91
	S2	L0.7W	1	1	0.7
		L72W	1	100	72
N = 1g	S3	L134M	468	0.4	134
D_r = 47%	S4	L256M	356	1	256
γ' = 9.9		L25564M	356	100	25564
kN/m^3					
N = 50g		C0.1W	1	0.1	0.1
D_r = 79%	S5	C1W	1	1	1
γ' = 10.47		C11W	1	10	11
kN/m^3					
N = 50g		C114M	679	0.15	114
D_r = 76%	S6	C764M	682	1	764
γ' = 10.41		C7361M	673	9.75	7361
kN/m^3		C41233M	669	55	41233

Note:
[1] S1 to S4: c_v = 5.58 x 10^{-5} m^2/s; S5 & S6: c_v = 3.57 x 10^{-5} m^2/s;

3 RESULTS AND DISCUSSIONS

3.1 Experimental results

The results of test conducted at N = 1g and 50g are presented in Figures 3 and 4 respectively, by plotting the bearing resistance (q_b), i.e. the measured force divided by footing area ($\pi d^2/4$), against the normalised depth (z/d). Good repeatability is observed between 2 pairs of repeated 1g tests at V ~ 0.7 and 70 respectively (Figure 3). At N = 50g, the two tests at the two highest V ≥ 7361 were stopped prematurely at z/d ~ 0.2, as the measured bearing resistance was approaching the capacity limit of the actuator to avoid damage to the equipment.

As shown in Figures 3 and 4, similar bearing resistance (q_b) and pore pressure (u) responses are observed at N = 1g and 50g. The q_b increases with increasing V, consistent with other rate effect studies in dilating sand (Chow et al., 2022) and with further discussion in Section 3.2.

The tests with $V \leq 7$ are drained in response based on the measured pore pressure response, while partially drained response is observed for $V > 7$. For tests between $7 < V < 25564$, positive excess pore pressure was measured initially for $z/d < 0.2$ before generation of negative excess pore pressure at deeper depths. The tests with $V \geq 25564$ exhibit only positive excess pore pressure for the penetration depth considered, although showing signs of transition toward negative excess pore pressure at greater depth. It is worth noting that the positive excess pore pressure (much less than the applied total stress) represents the true average penetration resistance at those depths and suggests dilation is still occurring, assuming essentially undrained conditions for these tests with $V \geq 25564$ (Chow et al., 2021).

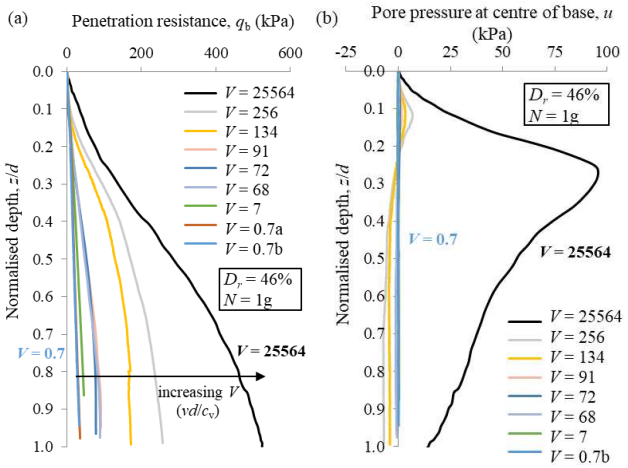

Figure 3. Model footing test results (N = 1g)

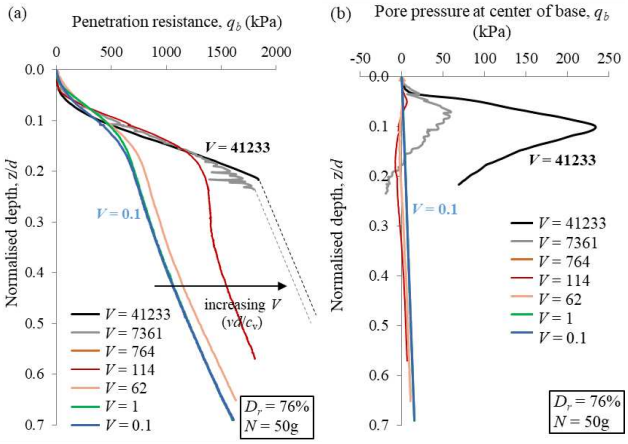

Figure 4. Centrifuge footing test results (N = 50g)

3.2 Rate effects in penetration resistance

The rate effect was determined by normalising the bearing resistance (q_b) at a given V with the reference drained bearing resistance $q_{b(dr,ref)}$ taken at v_{ref} = 0.001 m/s. To take into consideration the embedment depth effects, the $q_b/q_{b(dr,ref)}$ were determined over two z/d ranges of 0.06 to 0.12 (shallow embedment); and z/d = 0.4 to 0.7 (deep embedment) respectively. The shallow embedment range of z/d = 0.06 to 0.12 was selected for ease of comparison with existing rate effects study using a spudcan (Chow et al., 2021). The $q_b/q_{b(dr,ref)}$ were averaged at a z/d interval of 0.02 from z/d = 0.06 to 0.12 (Figure 5a); and a z/d interval of 0.1 from z/d = 0.4 to 0.7 (Figure 5b) respectively. The rate effect curves for these two z/d ranges can be captured using the backbone curve framework in Eq. (1):

$$\frac{q_b}{q_{b(dr,ref)}} = \left[\frac{1+(q_{b(un)}/q_{b(dr,ref)})(V/V_{50})^c}{1+(V/V_{50})^c}\right]\left[\frac{1+m[(v/d)/(v/d)_{ref}]^n}{1+m}\right] \quad (1)$$

where $q_{b(un)}$ is the undrained resistance at $V = V_{un}$, V_{50} is the non-dimensional velocity for 50% consolidation, and c, m and n are rate parameters respectively. The first term in Eq. (1) encapsulates the partial consolidation effects, while the second term captures the viscous rate effects (more details in Chow et al. 2022). Using non-linear least squares curve fitting technique, the fitted parameters for both ranges of z/d and N are summarised in Table 3. Note that the rate parameters at $z/d = 0.4$ to 0.7 were not fitted at $N = 50$g due to the missing data at the two highest V, caused by the penetration halt mentioned previously.

As shown in Table 3, similar rate parameters (c = 1.2, m = 0.35 and n = 0.03) can be fitted across the ranges of z/d and N considered. However, the non-dimensional velocity for 50% consolidation (V_{50}) varies between 230 and 2000 across the different z/d and N. The ratio of undrained to reference drained resistance, $q_{b(un)}/q_{b(dr,ref)}$ is also observed to increase with increasing embedment depth (z/d). At N = 1g, a significantly higher $q_{b(un)}/q_{b(dr,ref)}$ = 14.5 at z/d = 0.4 to 0.7 is observed as compared to $q_{b(un)}/q_{b(dr,ref)}$ = 5.8 at z/d = 0.06 to 0.12. On the other hand, $q_{b(un)}/q_{b(dr,ref)}$ increases with decreasing stress level (N), with $q_{b(un)}/q_{b(dr,ref)}$ = 5.8 (N = 1g) versus 1.09 (N = 50g). This highlights the need to consider the shallow embedment and stress level effects relevant for a given application.

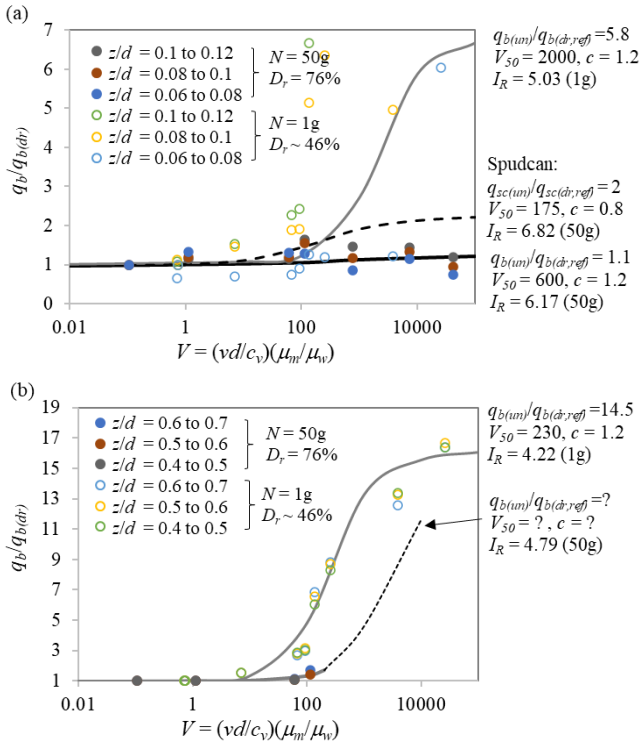

Figure 5. Quantification of rate effects using backbone curve for: (a) z/d = 0.06 to 0.12; (b) z/d = 0.4 to 0.7

The rate effects in circular footing are also compared against those reported in a centrifuge spudcan study in the same sand with D_r = 83% (see dashed line in Figure 5a, Chow et al., 2021). In the centrifuge spudcan study, the ratio $q_{sc(un)}/q_{sc(dr,ref)}$ = 2 was fitted from the shallow range of z/d = 0.08 to 0.12, versus $q_{b(un)}/q_{b(dr,ref)}$ = 1.09 (50g) for the circulate footing in the current study. The similar magnitude of rate parameters between the the spudcan and circular footing is not surprising given the similar compresive bearing mechanism under the spudcan and footing.

4 STRESS LEVEL EFFECTS

Figure 6a shows the comparison in drained penetration resistance between the 1g (Test L0.7W, D_r = 45%) and 50g tests (Test C0.1W, D_r = 76%) conducted in water saturated samples with the slowest V. Repeat tests at the two stress levels are also included in Figure 6a to demonstrate their repeatability. To provide insights into the stress level effects, the penetration resistance and depth are reproduced in dimensionless form as normalised resistance (q_b/σ'_v where σ'_v is the vertical effective stress) and normalised depth $(z/d).(p_a/d\gamma')^{0.5}$ where p_a is the atmospheric pressure and γ' is the effective unit weight) as shown in Figure 6b, similar to Richard et al. (2021). However, the q_b/σ'_v profiles of the 1g/45% and 50g/76% tests do not fall within a tight band as expected, instead the 50g/76% test produces a higher q_b/σ'_v profile than the 1g/45% test (Figure 6b). To aid the comparison, another 50g test involving loose sand (Test C0.6W, D_r = 30%) is included in Figure 6b and found to fall below the 50g/76% and 1g/45% tests. Further dimensional analysis is desired to establish a suitable dimensionless form which may resolve the issue.

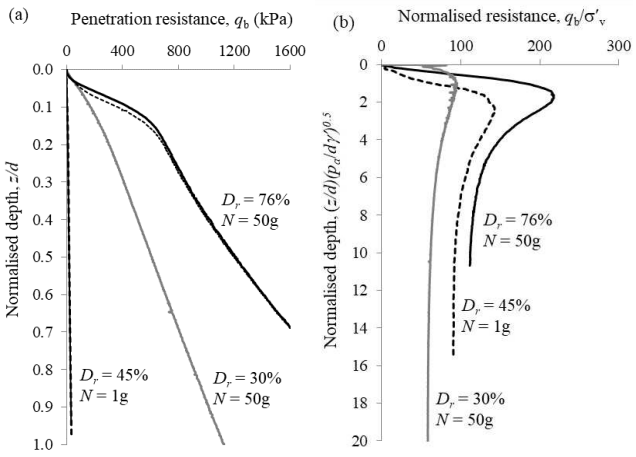

Figure 6. Stress level effects in circular footing tests.

Table 3. Fitted rate parameters

Application	N (g)	z/d range	$I_{R(avg)}$	d (m)	c_v (m^2/s)	D_r (%)	V_{dr}	V_{un}	$q_{(un)}/q_{(dr,ref)}$	V_{50}	c	m	n
Circular footing (this study)	1	0.06 to 0.12	5.03	0.04	5.58×10^{-5}	46	7	25000	5.8	2000	1.2	0.35	0.03
		0.4 to 0.7	4.22						14.5	230	1.2	0.35	0.03
	50	0.06 to 0.12	6.17	0.04	3.57×10^{-5}	76	10	-	1.09	600	1.2	0.35	0.03
Spudcan (Chow et al. 2021)	50	0.06 to 0.12	6.82	0.06	9.81×10^{-5}	83	6	4000	2	175	0.8	0.35	0.03

Table 4. Stress scaling approaches

Method	Formulation	Parameter*	$D_{r,1g}$	$D_{r,50g}$
Equivalent I_R	$I_R = D_r(Q - \ln p') - R = 4.54$ (Bolton, 1986)	$Q = 9.63$ $R = 1$	45%	76%
	$I_R = 5D_r - 1 = 2.8$ (Bolton, 1987)		76%	76%
Equivalent ψ	$v = \Gamma - \lambda \ln p'$ (Roscoe et al., 1958)	$\Gamma = 0.764$ $\lambda = 0.009$	61%	76%
	$e_{cs} = \Gamma - \lambda\left(\frac{p'}{P_{at}}\right)^{\xi}$ (Li & Wang, 1998)	$\xi = 0.7$ $\Gamma = 0.732$ $\lambda = 0.009$	76%	76%

** derived from triaxial tests (Chow et al., 2019)*

Figure 6b highlights the uncertainty in the stress scaling approach by maintaining an equivalent sand dilatancy between the 1g and 50g tests. The uncertainty arises from the conflicting treatment of stress-level dependency in existing stress-dilatancy relations at low stress levels (or mean stress, $p' < 150$ kPa). This is particularly relevant to the stress level in this study ($p' = 0.07$ and 6.7 kPa at 1g and 50g respectively at $z/d = 0.5$). As summarised in Table 4, this study adopted the Bolton (1986) relative dilatancy index ($I_R = D_r[Q - \ln p'] - R$), similar to the stress-scaling approaches reported in other studies (e.g. LeBlanc et al., 2010, Bradshaw et al., 2016). On the other hand, Bolton (1987) proposed an alternative relative dilatancy index ($I_R = 5D_r - 1$) that is independent of stress level for $p' < 150$ kPa, and which is supported by more recent studies (e.g. Richard et al., 2021). Adopting the Bolton (1987) I_R would mean the stress level effect is negligible here with $p' < 150$ kPa, and no scaling in D_r is required. This may explain why the normalised resistance for the 1g/45% in Figure 6b falls between the 50g/76% and 50g/30% tests.

Other than the equivalent I_R approach, stress level effects can also be addressed by maintaining an equivalent state parameter, ψ (Altaee and Fellenius, 1994). This approach is less popular due to the known difficulties in accurate determination of the critical state line (CSL) in the volumetric space. As shown in Table 4, depending on the CSL formulation, the 1g test could be modelled either at D_r = 61% (semi-logarithmic) or D_r = 76% (power-law), further highlighting the uncertainty in existing stress scaling approaches.

5 CONCLUSIONS

The penetration resistance of a circular footing in sand is shown to increase between 1.1 and 14.5 times when the consolidation condition changes from drained to undrained in the 1g and 50g model tests, spanning across 6 orders of magnitude increase in non-dimensional velocity (V) in dilating sand. The rate effects are found to increase with increasing normalised depth (z/d), but decreasing stress level (N). It is uncertain whether the high ratio of $q_{b(un)}/q_{b(dr,ref)}$ = 14.5 is caused by the significant dilation of the sand at low stress level in the 1g model tests, despite a stress scaling approach being applied to produce an equivalent dilatancy as field condition using the Bolton (1986)'s relative dilatancy index I_R framework. The disagreement between the 1g and 50g tests has revealed the limitation of existing stress scaling approaches, due to uncertainty in stress-dilatancy relation at low stress level (Table 4). More work is needed to establish a reliable strength-dilatancy relation for sand at low stress-level (e.g. using element tests), followed by validation using new 1g and 50g footing tests, applying the new stress-dilatancy relation.

AUTHOR CONTRIBUTION STATEMENT

S.H. Chow: Conceptualization, Methodology, Validation, Investigation, Data curation, Formal Analysis, Visualization, Writing-Original draft. **B. Bienen**: Methodology, Supervision, Writing-Reviewing and Editing. **M.F. Randolph**: Methodology, Writing-Reviewing and Editing, **T. Continibali**: Methodology, Investigation. Formal Analysis.

ACKNOWLEDGEMENTS

This research is funded by the Australian Research Council Discovery Grant Scheme (DP190100914).

REFERENCES

Altaee, A. and Fellenius, B.H. (1994). Physical modelling in sand. *Can. Geotech. J.* 31:420-431.

Bolton, M.D. (1986). The strength and dilatancy of sands. *Géotechnique* 36(1): 65–78.

Bolton, M.D. (1987). Discussion: the strength and dilatancy of sands. *Géotechnique* 37(2):219-226.

Bolton, M. and Gui, M. (1993). The study of relative density and boundary effects for cone penetration tests in centrifuge, University of Cambridge, Department of Engineering

Bransby, M.F. and Ireland, J. (2009). Rate effects during pipeline upheaval buckling in sand. *ICE Geo. Eng.* 162(5): 247–256.

Bradshaw, A. S., Giampa, J. R., Gerkus, H., Jalilvand, S., Fanning, J., Nanda, S., Gilbert, R., Gavin, K., and Sivakumar, V. (2016). Scaling Considerations for 1-g Model Horizontal Plate Anchor Tests in Sand, *Geotech. Testing J.* 39(6): 1006–1014.

Chow, S.H., Bienen, B. and Randolph, M.F. (2018). Rapid penetration of piezocones in sand. *Proc. 4th Int. Symp. on Cone Penetration Testing (CPT'18)*, Delft, 213-219.

Chow, S.H., Roy, A., Herduin, M., Heins, E., King, L. Bienen, B., O'Loughlin, C.D., Gaudin, C. and Cassidy, M.J. (2019). *Characterisation of UWA superfine silica sand*. Technical Report, The University of Western Australia, Geo 18844. https://doi.org/10.26182/5d8c185bcd366.

Chow, S.H., Bienen, B. and Randolph, M.F. (2021). Rapid penetration of spudcans in sand. *Proc. 4th Int. Symp. on Frontiers in Offshore Geotechnics.* Deep Foundations Institute, 2238-2247.

Chow, S.H., Bienen, B., Randolph, M.F. and Roy, A. (2022). Rapid soil-structure interactions in saturated sand. *Proc. 20th Int. Conf. on Soil Mechanics & Geo. Eng.* Accepted on 16/11/21.

Dow (2002). *Methocel Cellulose Ethers: Technical Handbook*. The Dow Chemical Company, Staines, UK.

Finnie, I.M.S. and Randolph, M.F. (1994). Punch-through and liquefaction induced failure of shallow foundations on calcareous sediments. *Proc. Int. Conf. on Behaviour of Offshore Structures*. Boston, MA, 217 – 230.

Leblanc, C., Houlsby, G.T. and Byrne, B.W. (2010). Response of stiff piles in sand to long-term cyclic lateral loading, *Géotechnique* 60(2): 79–90.

Li, X.S. and Wang, Y. (1998). Linear Representation of Steady-State Line for Sand. *J. Geotech. Geoenviron. Eng.*, 124(12): 1215–1217.

Palmer, A.C. (1999). Speed effects in cutting and ploughing. *Géotechnique* 49(3): 285–294.

Richard, I.A., Bransby, M.F., Byrne, B.W. and Gaudin, C. (2021) Effect of Stress Level on Response of Model Monopile to Cyclic Lateral Loading in Sand, *J. Geotech. Geoenviron. Eng.*, 147(3): 04021002.

Robinson, S., Brown, M.J., Matsui, H., Brennan, A., Augarde, C.E., Coombs, W. and Cortis, M. (2018). Centrifuge testing to verify scaling of offshore pipeline ploughs. *Int. J. of Physical Modelling in Geotechnics* 19(6): 305-317.

Roscoe, K.H., Schofield, A.N. and Wroth, C.P. (1958). On the yielding of soils. *Géotechnique* 8(1): 22–52.

INTERNATIONAL SOCIETY FOR SOIL MECHANICS AND GEOTECHNICAL ENGINEERING

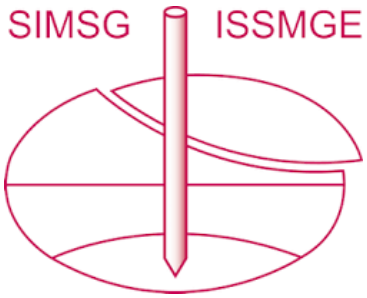

This paper was downloaded from the Online Library of the International Society for Soil Mechanics and Geotechnical Engineering (ISSMGE). The library is available here:

https://www.issmge.org/publications/online-library

This is an open-access database that archives thousands of papers published under the Auspices of the ISSMGE and maintained by the Innovation and Development Committee of ISSMGE.

The paper was published in the proceedings of the 5th International Symposium on Frontiers in Offshore Geotechnics (ISFOG2025) and was edited by Christelle Abadie, Zheng Li, Matthieu Blanc and Luc Thorel. The conference was held from June 9th to June 13th 2025 in Nantes, France.